

Xylitol acts as an anticancer monosaccharide to induce selective cancer death via regulation of the glutathione level

Nahoko Tomonobu^a, Ni Luh Gede Yoni Komalasari^{a,b}, I Wayan Sumardika^{a,b}, Fan Jiang^a, Youyi Chen^a, Ken-ichi Yamamoto^a, Rie Kinoshita^a, Hitoshi Murata^a, Yusuke Inoue^c, Masakiyo Sakaguchi^{a,*}

^a Department of Cell Biology, Okayama University Graduate School of Medicine, Dentistry and Pharmaceutical Sciences, 2-5-1 Shikata-cho, Kita-ku, Okayama-shi, Okayama, 700-8558, Japan

^b Faculty of Medicine, Udayana University, Denpasar, 80232, Bali, Indonesia

^c Faculty of Science and Technology, Division of Molecular Science, Gunma University, 1-5-1 Tenjin-cho, Kiryu-shi, Gunma, 376-8515, Japan

ARTICLE INFO

Keywords:

Xylitol
Cancer
Glutathione
ER stress
Chemotherapy

ABSTRACT

Herbal medicines and their bioactive compounds are increasingly being recognized as useful drugs for cancer treatments. The parasitic fungus *Cordyceps militaris* is an attractive anticancer herbal since it shows very powerful anticancer activity due to its phytochemical cordycepin. We previously discovered and reported that a high amount of xylitol is present in *Cordyceps militaris* extract, and that xylitol unexpectedly showed anticancer activity in a cancer-selective manner. We thus hypothesized that xylitol could become a useful supplement to help prevent various cancers, if we can clarify the specific machinery by which xylitol induces cancer cell death. It is also unclear whether xylitol acts on cancer suppression *in vivo* as well as *in vitro*. Here we show for the first time that induction of the glutathione-degrading enzyme CHAC1 is the main cause of xylitol-induced apoptotic cell death in cancer cells. The induction of CHAC1 is required for the endoplasmic reticulum (ER) stress that is triggered by xylitol in cancer cells, and is linked to a second induction of oxidative stress in the treated cells, and eventually leads to apoptotic cell death. Our *in vivo* approach also demonstrated that an intravenous injection of xylitol had a tumor-suppressing effect in mice, to which the xylitol-triggered ER stress also greatly contributed. We also observed that xylitol efficiently sensitized cancer cells to chemotherapeutic drugs. Based on our findings, a chemotherapeutic strategy combined with xylitol might improve the outcomes of patients facing cancer.

1. Introduction

Cancers remain a life-threatening disease. The consumption of foods or supplements that supply safe anticancer ingredients on a daily basis may help prevent the development of cancers by contributing to the body's cancer resistance. Some compounds may also be useful even when cancer emerges. We have been searching for new and effective anticancer components among traditional Asian medicines, and we have been focusing on the parasitic fungus *Cordyceps militaris*, a renowned anticancer herbal medicine [1,2]. *Cordyceps militaris* exhibits a very strong anticancer property [3] that is exerted by a well-known compound, cordycepin [4, 5], and possibly also several unknown components functioning in a cooperative manner.

We previously identified the anticancer monosaccharide xylitol in

an extract of *Cordyceps militaris* [2], and we observed that xylitol-mediated apoptosis occurred in a cancer-selective manner [2]. We therefore hypothesized that xylitol could be an effective and useful daily food component for preventing cancer and lessening cancer aggressiveness, as xylitol is not expensive (unlike cordycepin); xylitol is also readily available and is already used in food products worldwide, indicating a high level of safety.

However, it remains to be explained how xylitol triggers cancer-specific apoptosis at the molecular level. It is also not clear whether xylitol acts in an *in vivo* context for its anticancer ability; our previous work is limited to *in vitro* approaches. We conducted the present study to investigate potential mechanism(s) of xylitol-mediated cancer death and the usefulness of xylitol *in vivo*.

* Corresponding author.

E-mail address: masa-s@md.okayama-u.ac.jp (M. Sakaguchi).

<https://doi.org/10.1016/j.cbi.2020.109085>

Received 28 January 2020; Received in revised form 19 March 2020; Accepted 2 April 2020

Available online 07 April 2020

0009-2797/© 2020 The Authors. Published by Elsevier B.V. This is an open access article under the CC BY license (<http://creativecommons.org/licenses/by/4.0/>).

Abbreviations

ATF4	activating transcription factor 4	GSH	glutathione
ATF6	activating transcription factor 6	GAPDH	glyceraldehyde-3-phosphate dehydrogenase
ATP	adenosine-3'-triphosphate	HRP	horseradish peroxidase
BiP	binding-immunoglobulin protein	IRE1 α	inositol-requiring protein 1 alpha
CBB	coomassie brilliant blue	NAC	N-Acetyl-L-cysteine
CD44v	CD44 variant isoform	PAGE	polyacrylamide gel electrophoresis
CHAC1	ChaC glutathione specific gamma-glutamylcyclotransferase 1	PERK	PKR-like ER kinase
EMSA	electrophoretic mobility shift assay	PVDF	polyvinylidene difluoride
ER	endoplasmic reticulum	ROS	reactive oxygen species
5-FU	5-fluorouracil	RT-PCR	reverse transcription-polymerase chain reaction
		SDS	sodium dodecyl sulfate
		TUDCA	tauroursodeoxycholate

2. Materials and methods**2.1. Cell lines and chemicals**

HEK293T cells (embryonic kidney cells stably expressing the SV40 large T antigen), MeWo cells (a human melanoma cell line), and PANC-1 cells (a human pancreatic cancer cell line) were obtained from the American Type Culture Collection (Manassas, VA). Normal human OUMS-24 fibroblasts were established by Dr. Masayoshi Namba [6]. These human cells were all cultivated in D/F medium (Thermo Fisher Scientific, Waltham, MA) supplemented with 10% fetal bovine serum (FBS) in a humidified incubator filled with 5% CO₂ at 37 °C.

The chemicals used in this study were as follows: xylitol (Wako, Hiroshima, Japan), tauroursodeoxycholate (TUDCA) (Sigma-Aldrich, St. Louis, MO), 5-fluorouracil (5-FU) (Sigma-Aldrich), dacarbazine (Tokyo Chemical Industry, Tokyo), and N-Acetyl-L-cysteine (NAC) (Tokyo Chemical Industry).

2.2. RNA-seq analysis

To identify gene(s) that play a role in xylitol-mediated apoptotic cell death in cancer cells, we performed an RNA-seq-based comprehensive analysis of gene expressions in MeWo cells that were treated or not treated with xylitol, and we compared the altered gene expressions among them. Total RNA was extracted from cells with ISOGEN (Nippon Gene, Tokyo) according to the manufacturer's instructions. The isolated RNA was subjected to an RNA-seq-based comprehensive analysis of gene expression (Bioengineering Lab, Kanagawa, Japan).

2.3. Quantitative real-time PCR analysis

To confirm the results of the RNAseq analysis of selected genes, we further investigated the genes' expression alterations caused by xylitol in MeWo cells by conducting a quantitative real-time PCR analysis. Total RNAs were extracted from the three cell lines with Isogen II (Wako). The prepared RNAs (500 ng) from cultured cells were changed to cDNAs by reverse-transcription with SuperScript™ II (Thermo Fisher Scientific). A real-time reverse transcription-polymerase chain reaction (RT-PCR) was performed by a LightCycler rapid thermal cycler system (ABI 7900HT; Applied Biosystems, Foster City, CA) using a LightCycler 480 SYBR Green I Master (Roche Diagnostics, Indianapolis, IN). The levels of mRNA expression were normalized relative to *TBP* mRNA as an internal control, using the $\Delta\Delta C_t$ method.

The following forward and reverse primer pairs (5' to 3') were used: *CHAC1* (forward: AGGGAGACACCTTCCATCG; reverse: CTCCCCTTGCACTTGATG), *HIPK2* (forward: CAGCACCAGTCATCTGTGAGA; reverse: TCTCCTTGACACGCTTGGAT), *MAFK* (forward: CCAAACCGAATAAGGCATTAAG; reverse: CCTCCTCTGGTGAGACC), *RERE* (forward: CACCTCCACCAGCAGGAC; reverse: GAGGGTTGGGAGAGTGTC), *BCAP29* (forward: TTTTGGAAACAAGGCTTCC; reverse: GGTGGAGCTCTTCTCAA

TGG), *MRPL34* (forward: TCAAACGCAAGAACAAGCAC; reverse: AATGCTCAGCGACTTGC), *PIR* (forward: ACAGCAGTGTGGAGAAGG; reverse: GCTCCCAGCAATTAAGACA), *RPP21* (forward: CTCTCTGTGCGAGGCTGCTCT; reverse: GGCATGTTAGGCAGGTCTGT), *TBP* (forward: GAACATCATGGATCAGAACAACA; reverse: ATAGGGATTCCGGGAGTCAT).

2.4. siRNA

To examine the possible role(s) of CHAC1 in cancer cells, we performed RNA interference experiments. Human CHAC1 siRNA (siCHAC1 #0, sense: CCCAUACUGUUACCAUAAtt and antisense: UUAUGGGUAACAGUAUUGGgac; siCHAC1 #1, sense: CUACUUGAAACUUUUUUAtt and antisense: UAAAUAAAAGUUUCAAGUAGta; siCHAC1 #2, sense: GGCUGGAUGAGGGAAUAGUAtt and antisense: UACUAUCCCUCAUCCA GCctg) and control siRNA (control glyceraldehyde-3-phosphate dehydrogenase (GAPDH) siRNA, sense: UGGUUUACAUGUUCCAAUAtt and antisense: UAUUGGAACAUGUAAACCAAtg) were purchased from Thermo Fisher Scientific. Each siRNA was transfected to the cells using Lipofectamine RNAiMAX reagent (Thermo Fisher Scientific) at a final concentration of 10 nM in culture. After 24-h exposure to the transfection mixture, the gene-silencing efficiency of the cells was measured by a quantitative real-time PCR analysis.

2.5. Western blotting

To determine the protein expression levels of interest in the cells and tissues, we carried out a Western blot analysis. The collected cell pellets were lysed by pipetting in ice-cold M-PER buffer (Thermo Fisher Scientific) and kept on ice for 30 min. The tumor tissues dissected from mice were thoroughly homogenized by a homogenizer (UD-201; Tomy Seiko, Tokyo) and kept on ice for another 30 min. After centrifugation of the suspensions at 15,000 rpm for 20 min, the clear supernatants were prepared as whole protein lysates.

The protein concentrations of all the prepared whole lysates were measured according to the Bradford method using a Bio-Rad protein assay kit (Bio-Rad Laboratories, Hercules, CA). A total of 10 μ g of protein lysate was loaded onto a 12% sodium dodecyl sulfate-polyacrylamide gel electrophoresis (SDS-PAGE) gel, separated according to the molecular weights, and transferred to polyvinylidene difluoride (PVDF) membranes. The membranes were blocked with 10% skim-milk/PBST for 1 h at room temperature, and then incubated with the following primary antibodies at 4 °C overnight: rabbit anti-human CHAC1 (Proteintech, Tokyo), rabbit anti-human binding immunoglobulin protein (BiP) (Cell Signaling Technology, Danvers, MA), rabbit anti-human cleaved caspase-3 (Asp175) (Cell Signaling Technology) or mouse anti-human α -tubulin (Sigma-Aldrich) followed by incubation with secondary antibodies (horseradish peroxidase [HRP]-conjugated anti-mouse or anti-rabbit IgG antibody [Cell Signaling Technology]) at room temperature for 1 h.

Target protein bands were visualized on x-ray film that covered the reacted PVDF membrane with a chemiluminescence system (Pierce ECL Plus, Thermo Fisher Scientific). Considering the nature of the experimental settings and the specimens used, either detection of tubulin with western blotting or total protein staining of the SDS-PAGE gels with Coomassie brilliant blue (CBB) was used as a loading control.

2.6. Electrophoretic mobility shift assay (EMSA)

We performed an electrophoretic mobility shift assay (EMSA) to investigate the possible mechanism and the role of the selected transcription factors, i.e., ATF4 and NFκB. Nuclear extracts from MeWo cells were prepared in accord with the manufacturer's instructions, using NE-PER Nuclear Extraction Reagent (Thermo Fisher Scientific). The protein concentrations of the prepared nuclear extracts were measured according to the Bradford method as described above in the Western blotting section. The 5'-biotin-labeled double-stranded probes (ATF4: forward: 5'-aaGGATGATGCAATAcc-3' and reverse: 3'-ggTATTGCATCATCctt-5'; NFκB: forward: 5'-agttgaGGGACTTCCcagc-3' and reverse: 3'-gcctgGGAAAGTCCCtcaact-5') were purchased from Sigma-Aldrich.

The DNA probes were mixed with 2 μg of crude nuclear extracts in a reaction mixture (20 μl) containing 60 mM KCl, 5 mM MgCl₂, 0.1 mM EDTA, 1 μg of poly (dI-dC), 1 mM dithiothreitol, 5% glycerol, and 20 mM HEPES (pH 7.9) and incubated on ice for 30 min. DNA-protein complexes were then separated by electrophoresis in a 7% polyacrylamide gel (PAGE) under non-denaturing conditions and blotted onto a Biotodyne B nylon membrane (Pall, Tokyo). The bands were detected using a LightShift Chemiluminescent EMSA kit (Thermo Fisher Scientific) according to the manufacturer's instructions.

2.7. Evaluation of cellular apoptosis, ROS, glutathione, and ATP

To evaluate apoptotic cell death and its related oxidative stress, we conducted the following assays. Apoptotic cells were detected as described previously [1,2]. Briefly, a cell culture stained with Hoechst33342 solution (Thermo Fisher Scientific) at a final concentration of 5 μg/ml was incubated for 30 min. We then used fluorescence microscopy to observe apoptotic cells that showed markedly high brightness with Hoechst staining due to the apoptosis-induced shrinking of their nuclei, which could be readily distinguished from the nuclei of non-apoptotic cells. Each well was microscopically imaged in five distinct regions at 200 × magnification in triplicate. The numbers of apoptotic cells (showing bright blue fluorescence) and total cells (apoptotic cells and non-apoptotic cells showing dark blue fluorescence) to the five non-overlapping regions were counted and then summed as the total apoptotic cell number and the total cell number, respectively. The numbers of apoptotic cells are presented as the averages of the percentages of all cells from three independent experiments. Cellular apoptosis was evaluated by the detection of cleaved caspase-3 by western blotting (see the Western blotting section). The intracellular levels of reactive oxygen species (ROS), glutathione (reduced type: GSH), and adenosine-3'-triphosphate (ATP) were measured by using the following respective kits: the ROS Detection Cell-Based Assay Kit (DHE) (Cayman Chemical, Ann Arbor, MI), the Amplitude™ Fluorimetric Glutathione Assay Kit Green Fluorescence (AAT Bioquest, Sunnyvale, CA), and the ATP Detection Assay Kit-Luminescence (Cayman Chemical).

2.8. Animal experiments

To expand the *in vitro* study of xylitol to an *in vivo* investigation, we carried out an evaluation of the anticancer effect(s) of xylitol on a cancer-bearing mouse model. The experimental protocols were approved by the Animal Experiment Committee at Okayama University (approval no. OKU-2017250). All mouse procedures and euthanasia,

including cell transplantations, were done painlessly or with the mouse under anesthesia, within the Committee's strict guidelines.

For the evaluation of tumor growth *in vivo*, MeWo cells (2×10^6 cells) mixed with Matrigel were subcutaneously transplanted into the back on the right side of BALB/c-nu/nu mice (CLEA Japan, Tokyo). The size of each tumor was measured with Vernier calipers, and the tumor volume was calculated as $1/2 \times (\text{shortest dia.})^2 \times (\text{longest dia.})$. For a series of xenograft experiments, all mice were randomly divided into two groups (Fig. 4) or four groups (Fig. 5, 6A–D), at five mice per group.

2.9. Treatment procedure

We selected the doses of the chemicals used in this study by referring to the IC50 and LD50 values of these chemicals reported in scientific journals and the publicly available data provided by medical companies. For xylitol, these values were IC50 = 6.77% in A549 cells and 5.88% in HCT-115 cells [7], and LD50 > 4000 mg/kg per mouse (a single injection via the tail vein) [8]. For TUDCA, they were LD50 > 600–800 mg/kg per rat (a single injection via the tail vein) (<https://patentimages.storage.googleapis.com/f9/17/63/c83e303b27c9d4/EP0773029A1.pdf>). For 5-FU, they were IC50 = 50 μg/ml in MeWo cells [9], and LD50 > 250 mg/kg per mouse (a single injection via the tail vein) (website: https://medical.kyowakirin.co.jp/site/drugpdf/interv/5fu_iv_in.pdf). For dacarbazine, they were IC50 = 500 μg/ml in MeWo cells [9], and LD50 > around 470 mg/kg per mouse (a single injection via the tail vein [10]). We set the chemical doses and their treatment-time schedules based on the above information.

In the *in vitro* culture system, cells were treated with xylitol in the range of 1 mg/ml (0.1%) to 50 mg/ml (5%) (final concentration) for either 24 or 48 h according to the experimental settings. Cells were also treated with dacarbazine (0 μM, 100 μM [18 μg/ml], or 500 μM [100 μg/ml]) with or without xylitol (25 mg/ml, 2.5%) for 48 h. The percentage of apoptotic cells in the control culture of the intact cells generally reaches approximately 10%. To more clearly show the effect of xylitol on the number of apoptotic cells, we added xylitol to the cultures just after the replacement with fresh medium to allow the removal of the apoptotic cells that were already present in the control cultures.

For the *in vivo* animal experiments, we used 2.0 g/kg of xylitol. The reason for this dose is as follows. The *in vitro* effective and maximum dose is 25 mg/ml. Given that the weight of one mouse is ~20 g, its total blood will be ~2 ml in volume so that the following is obtained: 25 mg/ml = 50 mg/2 ml (blood volume) = 50 mg/20 g (mouse weight). This ratio is comparable to 2.5 g/kg. Considering that differences between *in vitro* and *in vivo* environments may lead to unexpected side effects in a living body, we finally defined 2.0 g/kg as an applicable dose to each mouse after contemplating a slight reduction from the calculated dose (2.5 g/kg). The concentration 2.0 g/kg is one-half of the LD50 (4 g/kg) of xylitol per mouse as mentioned above.

For the treatment schedule, in consideration of a previous report describing the half-life of xylitol in rats as approx. 7–8 h [11], we decided to administer xylitol to the mice at the same dose ratio (2.0 g/kg) on a daily basis.

After a tumor had grown at the injected site to 50–100 mm³ in volume, either control phosphate-buffered saline (PBS) or xylitol (2.0 g/kg in PBS) was orally or intravenously administered daily to the mice. The ER-stress inhibitor sodium tauroursodeoxycholate (TUDCA; 250 mg/kg in PBS) [12, 13] was further injected intraperitoneally on day 7 and subsequently injected every other day in the same way.

2.10. Statistical analysis

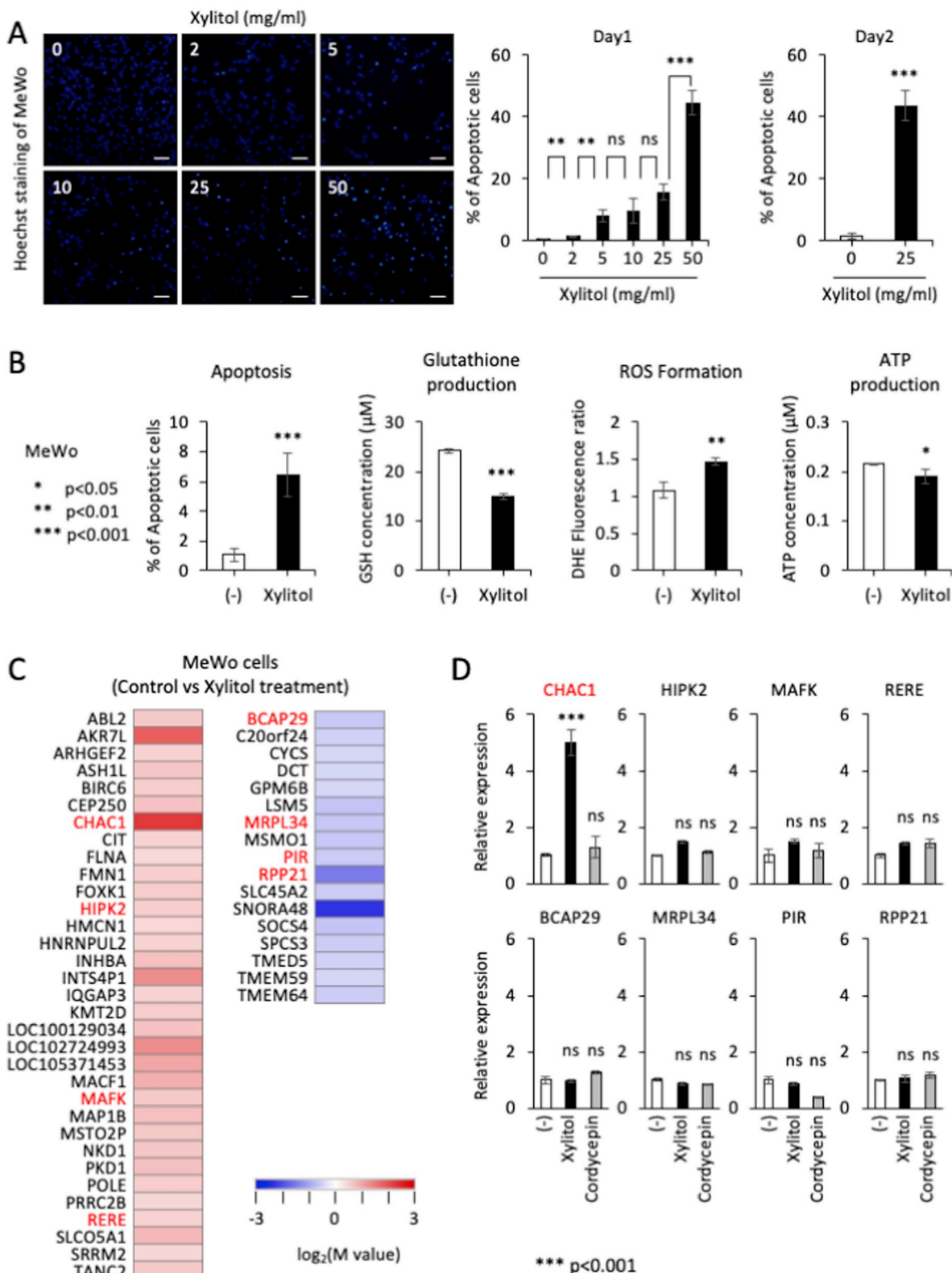
All values are expressed as the mean ± SD. All data were analyzed by unpaired Student's t-test for significant differences between the mean values of each group.

3. Results

3.1. Xylitol induced apoptotic cell death in cancer cells via oxidative stress

We previously reported that the xylitol content in our prepared *Cordyceps militaris* extract was 2.34 mg/ml [2]. In the present study,

therefore, we evaluated the dependence of the induction of the apoptosis of melanoma cells on the dose of xylitol, starting with 2 mg/ml as the lowest concentration. As shown in Fig. 1A, we confirmed that 24-h treatment with xylitol induced apoptotic cell death in MeWo cells in a dose-dependent manner. The 50 mg/ml dose showed the greatest effect in this context. In parallel with this experimental setting, the xylitol-



(caption on next page)

Fig. 1. The induction of the apoptotic cell death of MeWo cells by xylitol and the identification of CHAC1 as one of the top-rated genes relevant to the xylitol-mediated apoptosis. **A:** MeWo cells were treated with xylitol at 0–50 mg/ml for 24 h (left and middle). The detection of apoptotic cell death was achieved by Hoechst 33342 staining, which brings bright fluorescence to the cells displaying apoptotic nuclear shrinkage. *Left panel:* Cell-stained images at 24 h. Scale bars: 50 μ m. *Middle panel:* Quantified data from the counting of apoptotic cells at 24 h. *Right panel:* Quantified data from the counting of apoptotic cells at 48 h after treatment with xylitol (25 mg/ml). **B:** MeWo cells were treated with xylitol at a final conc. of 25 mg/ml for 24 h. Hoechst-based counting of apoptotic cells and measurements of cellular glutathione, ROS, and ATP were performed. **C:** Heat maps from the data of RNA-seq are displayed for the picked-up genes that were up- and downregulated in MeWo cells after xylitol treatment. These analyses were performed using the database for annotation, visualization and integrated discovery (DAVID) v6.8 (<http://david.ncicfr.gov/>). **D:** The mRNA expression of the selected genes relative to TBP as the internal control were evaluated in MeWo cells, which were not treated or were treated with xylitol or cordycepin as determined by qRT-PCR. Data are mean \pm SD. ns, not significant; * $p < 0.05$, ** $p < 0.01$, *** $p < 0.001$ by Student's *t*-test.

mediated apoptosis in MeWo cells was also confirmed by another method, i.e., the western blot-based detection of the cleaved caspase-3. By this approach, we confirmed that the cleaved caspase-3 was present in the cell extracts treated with 5 mg/ml of xylitol, and the detected band was further increased in a dose-dependent manner (Supplementary Fig. S1).

Although 50 mg/ml of glucose could not induce apoptosis in MeWo cells (data not shown) due to the somewhat high osmotic pressure for 50 mg/ml (329 mOsm/L) compared to physiological pressure (285 \pm 5 mOsm/L), we decided to use 25 mg/ml as the highest xylitol dose in a series of *in vitro* experiments. The xylitol-mediated apoptotic cell death was further enhanced by treatment with xylitol for another 48 h, to a significant level (Fig. 1A). To obtain insights into the cellular events relevant to this xylitol-induced apoptosis, we then examined the cellular oxidative state, since it is closely associated with the cellular apoptotic process in many physiological scenarios. As we expected, the apoptosis induced by 25 mg/ml of xylitol was followed by a marked elevation of ROS (Fig. 1B). In parallel with this, the reduced glutathione (GSH) level was also significantly reduced, whereas the ATP showed only a slight reduction. The xylitol-mediated reduction of the GSH level was further confirmed by another method (Supplementary Fig. S2). Interestingly, the xylitol-mediated apoptotic cell death was significantly attenuated by the pretreatment with an ROS inhibitor, NAC (Supplementary Fig. S3), suggesting that ROS are highly involved in the xylitol-mediated apoptotic process of cancer cells.

In light of these cellular events, we next sought to identify key gene (s) that may play a critical role in the xylitol-mediated cancer death. The results of the RNA-seq analysis (Fig. 1C) revealed several genes of interest. We focused on the genes marked in red in Fig. 1 because these selected genes are highly associated with apoptotic events that occur with the regulation of oxidative stress, and with mitochondria, DNA replication, and protein translation. The genes are as follows. *CHAC1*: Regulates glutathione levels and oxidative balance in cells. *HIPK2*: Inhibits cell growth and promotes apoptosis through the activation of p53. *MAFK*: Functions as a transcriptional regulator in response to oxidative stress. *RERE*: Functions as a transcriptional regulator in response to oxidative stress. *BCAP29*: Involved in CASP8-mediated apoptosis. *MRPL34*: Functions as a mitochondrial ribosome. *PIR*: Involved in the regulation of DNA transcription and replication. *RPP21*: Generates mature tRNA molecules by cleaving their 5-ends.

As we noted in the Introduction section, *Cordyceps militaris* exhibits a very strong anticancer property [3] due to two of its constituent compounds, xylitol [2] and the well-known cordycepin [4, 5]. To confirm the specific induction of these genes by xylitol, we next conducted a quantitative-real time PCR for the selected genes. The confirmation approach showed that the *CHAC1* gene was induced at a much higher level compared to both the not-treated and cordycepin-treated cases (Fig. 1D). We thus decided to focus on *CHAC1* as an important gene that may regulate apoptosis in response to xylitol but not cordycepin.

3.2. *CHAC1* plays a part in the xylitol-mediated cancer cell death

To test whether the xylitol-mediated apoptosis is limited to malignant MeWo cells (and does not affect normal cells), we investigated the effects of xylitol on another type of human cancer cells and on normal human fibroblasts. As shown in Fig. 2A, we observed that the human

pancreatic cancer PANC-1 cells showed an apoptotic phenotype like that of the MeWo cells after xylitol treatment, whereas OUMS-24 fibroblasts did not show any appreciable apoptotic phenotype. As shown in Fig. 2A, this selective apoptotic event in cancer cells was further confirmed by our similar independent experiments that included other pancreatic cancer cell lines, AsPC-1 and MIA PaCa-2 (Supplementary Fig. S4A). In addition, ROS were constantly induced at a significant level in the cancer cell lines, but the induction did not occur in the normal OUMS-24 cells (Supplementary Fig. S4B), and there was also no induction of apoptosis cells in the normal OUMS-24 cells (Supplementary Fig. S4A). Interestingly, the xylitol-mediated apoptotic event also matched the induction rate of *CHAC1* in all cell types examined, i.e., OUMS-24, MeWo and PANC-1 (Fig. 2B).

CHAC1 was next downregulated by an RNAi technique for the assessment of its relevance to apoptotic cell death. We first checked the effect of *CHAC1* siRNAs (siCHAC1 #0, #1 and #2; see the siRNA section above) on the downregulation of the intrinsic *CHAC1* expression in two cell lines, MeWo and HEK293T. The results revealed that, among the siRNAs used, siCHAC1 #1 caused the highest reduction of *CHAC1* (Fig. 2C). Because it was the most effective, we then treated cells with siCHAC1 #1 and found that the xylitol-induced apoptotic cell death was dramatically attenuated (Fig. 2D). The siRNA also caused a downregulation of the xylitol-mediated ROS production and inversely restored the glutathione level. The ATP level was not changed even after siRNA treatment. Considering that *CHAC1* is major glutathione-degrading enzyme [14], the xylitol-mediated increase in ROS is rational.

3.3. Xylitol induced ER stress

It has been reported that *CHAC1* induction is transcriptionally regulated by ATF4 via ER stress [14–16], and we therefore investigated the potential ability of xylitol to induce ER stress. An induction of the major ER chaperone, binding-immunoglobulin protein (BiP), is a reliable index marker for the observation of cellular events following ER stress. In non-stressed cells, BiP binds and inhibits three representative ER stress sensors: inositol-requiring protein 1 alpha (IRE1 α), activating transcription factor 6 (ATF6), and PKR-like ER kinase (PERK). Upon the induction of ER stress, BiP is recruited by the misfolded proteins and is subsequently released from the three sensors [17]. The resulting free sensors all undergo autoactivation and induce their own signaling cascades that are relevant to multiple cellular events of the ER stress. In this experimental setting, we thus sought to determine whether cells react to ER stress by evaluating the induction levels of BiP protein after treating the cells with xylitol.

As shown in Fig. 3A, xylitol but not glucose significantly induced BiP protein in parallel with *CHAC1* induction in a dose-dependent manner. In addition, when we used an ATF4-specific probe (Fig. 3B) to search for the ATF4 activation state after xylitol treatment, the results confirmed that ATF4 (Fig. 3C, left) but not NF κ B (Fig. 3C, right) was highly upregulated in response to xylitol, in a manner similar to the induction of BiP and *CHAC1* proteins (Fig. 3A).

3.4. Xylitol mitigated melanoma growth *in vivo* through ER stress

Since the results obtained thus far demonstrated that xylitol plays a part in selective cancer death *in vitro*, we next investigated whether

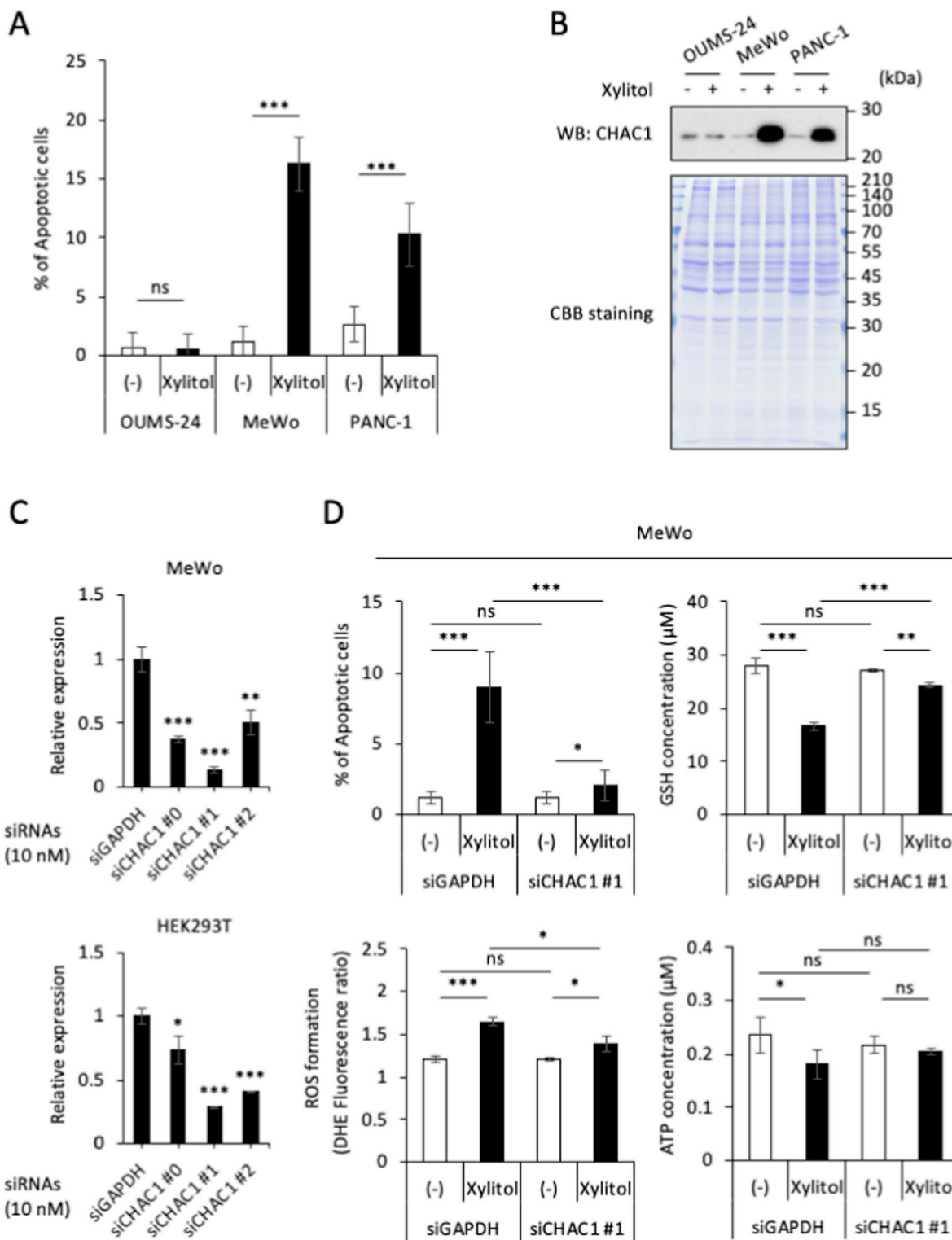


Fig. 2. The critical role of CHAC1 in xylitol-mediated apoptotic death in cancer cells. **A,B:** Human melanoma MeWo cells, human pancreatic PANC-1 cells, and normal human OUMS-24 fibroblasts were treated with xylitol at a final conc. of 25 mg/ml for 24 h. Apoptotic cells were detected by Hoechst staining and then quantified (**A**) and CHAC1 induction was detected by Western blot (**B**). **C:** The prepared CHAC1 siRNAs (#0, #1, #2) were checked for their downregulating effects on the intrinsic CHAC1. *Top:* MeWo cells. *Bottom:* HEK293T cells. **D:** MeWo cells were transfected with either siCHAC1 #1 or siGAPDH as a control for 24 h and then treated with xylitol at a final conc. of 25 mg/ml for another 24 h. Hoechst-based counting of apoptotic cells (*left-top panel*) and measurements of cellular glutathione (*right-top*), ROS (*left-bottom*) and ATP (*right-bottom*) were performed. Data are mean \pm SD. ns, not significant; *p < 0.05, **p < 0.01, ***p < 0.001 by Student's t-test.

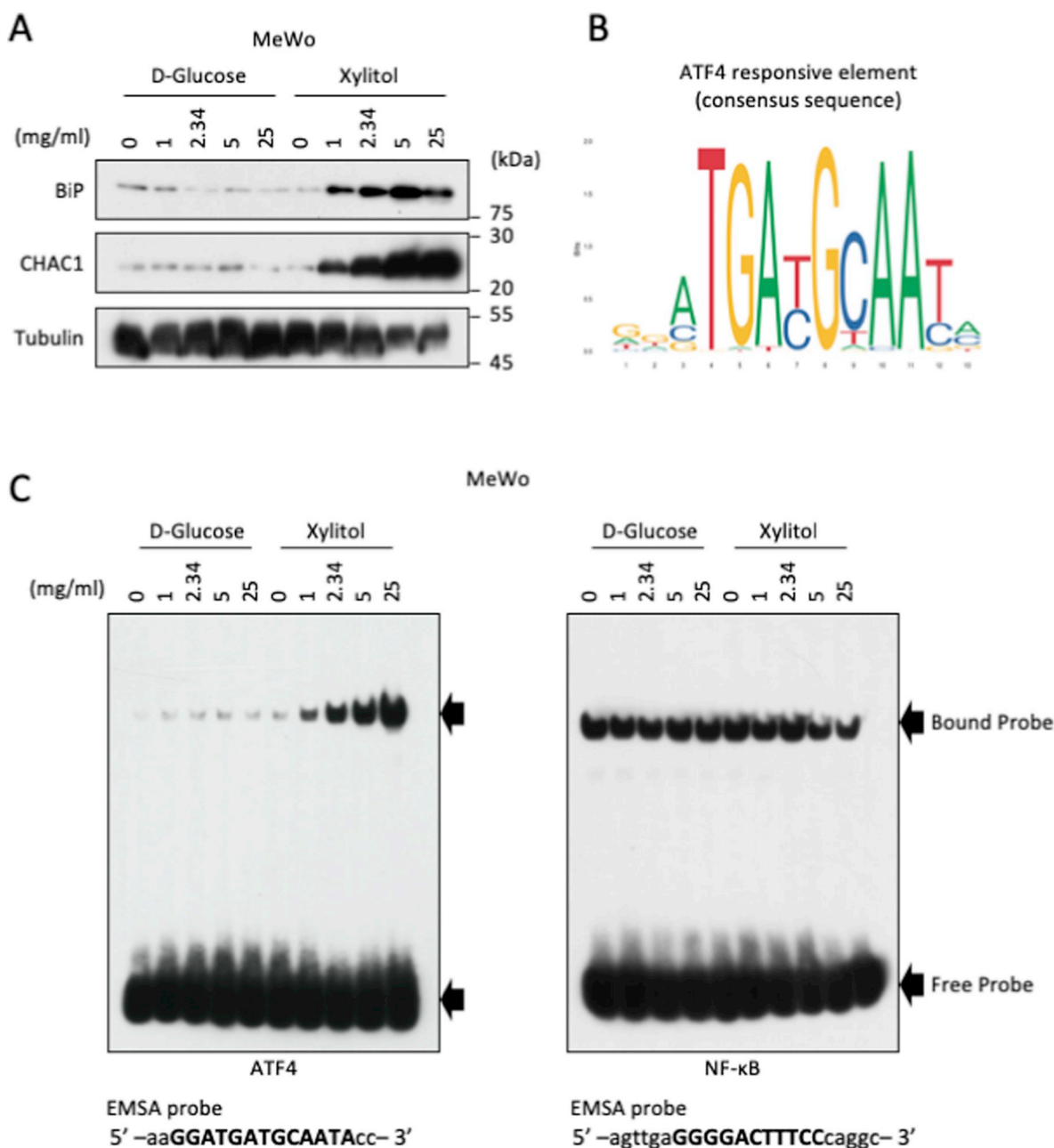


Fig. 3. The induction of CHAC1 by the xylitol-triggered ER-stress. **A:** MeWo cells were treated with glucose or xylitol at the indicated doses for 24 h. BiP and CHAC1 were detected by western blots using the prepared whole cell extracts. **B:** Consensus sequence of the ATF4 responsive cis-element (<http://jaspar.genereg.net/matrix/MA0833.1/>). **C:** EMSA was performed after the preparation of cell specimens under conditions similar to those described for panel (A) except for the use of nuclear extracts. *Left panel:* Detection of the ATF4 probe. *Right:* Detection of the NFκB probe.

xylitol also works *in vivo*. The administration route may be important for the appropriate action of xylitol against cancer *in vivo*, and we thus administered the same amount of xylitol by an oral route (Fig. 4A and B) and via the tail vein of mice (Fig. 4C–F). In these *in vivo* models, we used 2.0 g/kg because this dose is similar to the *in vitro* effective and maximum dose (25 mg/ml). We considered this dose safe, since the LD50 in mice is 10-fold higher than the selected dose at either an oral [8] or intravenous [8] route.

Because the half-life of xylitol in rats is approx. 7–8 h [11], we administered xylitol at the same dose to the mice on a daily basis. With this approach, we observed that the oral administration had no effect on the MeWo cell-derived tumor volume (Fig. 4A) or weight (Fig. 4B), whereas the intravenous injection attenuated the tumor growth rate (Fig. 4C). Throughout the monitoring period, the body weights of the

mice were not affected by the xylitol treatment (Fig. 4D). On day 15, we observed again that the tumor weights were actually decreased in the xylitol-treated group (Fig. 4E), and this was also true of the tumor volumes (Fig. 4C).

Like glucose, xylitol can also be used in glycolysis [18], which plays a fundamental role in cancer cell growth through the production of ATP energy. In the present experiment, the glycolysis occurred particularly in the tumor masses grown in an *in vivo* environment compared to the *in vitro* monolayer culture system, since inside of a tumor mass displays a high level of hypoxia. We therefore examined the glycolysis state of the xylitol-treated tumors (the MeWo cell-derived tumors) in a comparison with the control PBS-treated groups. The mass spectrometry-based analysis of metabolites showed no appreciable alterations of the major metabolites produced by glycolysis (Supplementary Fig. S5), suggesting

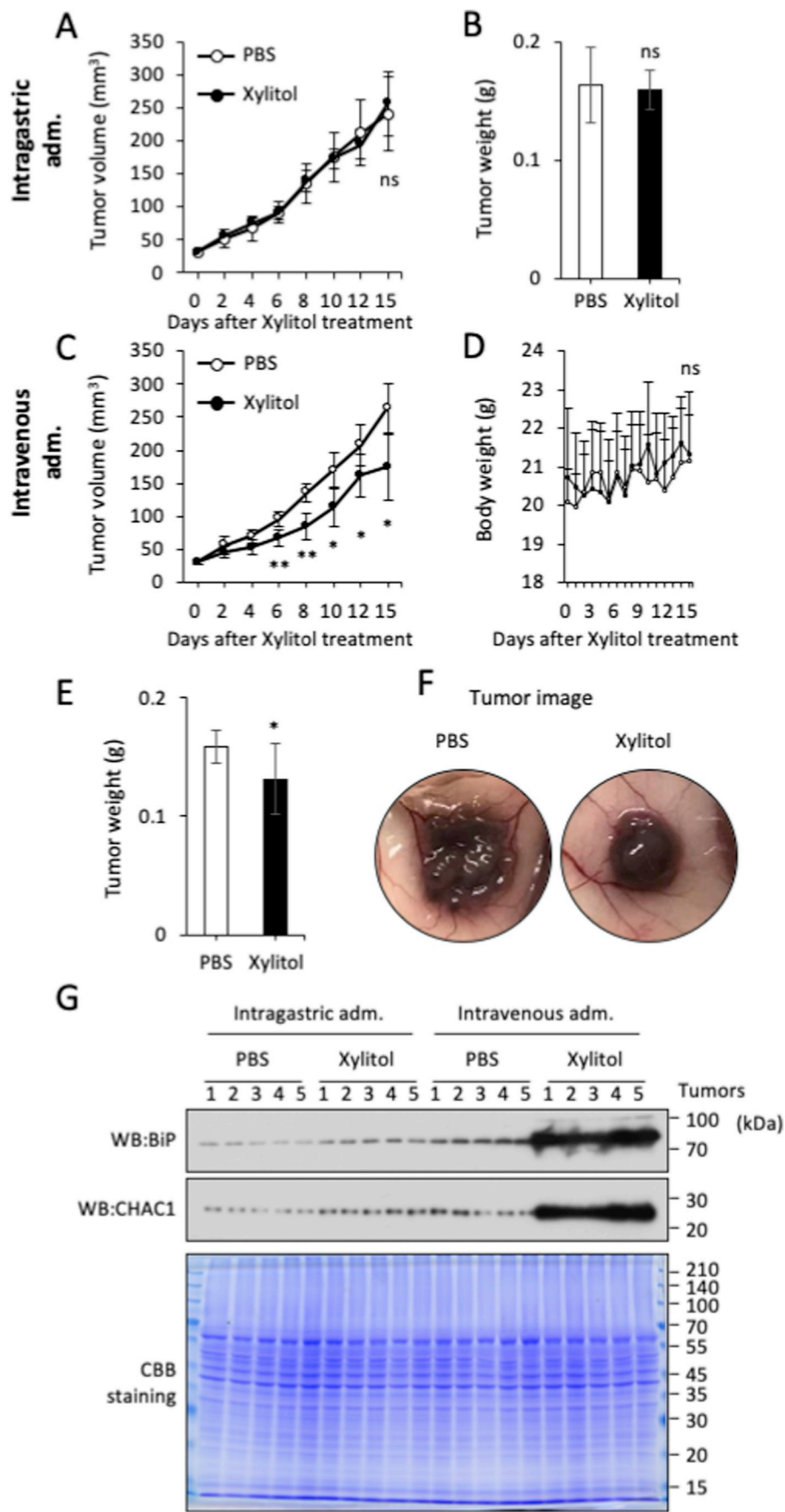


Fig. 4. The tumor-suppressive function of xylitol *in vivo*. **A,B:** MeWo cell-derived tumor sizes were monitored on the indicated days. Xylitol (2.0 g/kg in PBS, which corresponds to approx. 20 mg/ml *in vitro*) was orally administered starting at day 0 (the tumor volumes reached ~50–100 mm³) and then every day until the monitoring was discontinued (A). On day 15, the resected tumors were all weighed (B). **C–F:** MeWo cell-derived tumor sizes (C) and body weights (D) were monitored on the indicated days after the administration of xylitol (2.0 g/kg in PBS) by way of the tail vein starting at day 0 and then daily. Tumor weights were quantified (E) and tumor images were taken (F) 15 days after the administration. **G:** On day 15, the resected tumors were collected, lysed, and subjected to SDS-PAGE, and then the protein levels of BiP and CHAC1 were evaluated by western blots. *Bottom:* CBB staining showing the internal control and proper loading of the protein specimens. Data are mean ± SD. ns, not significant; *p < 0.05, **p < 0.01, ***p < 0.001 by Student's *t*-test.

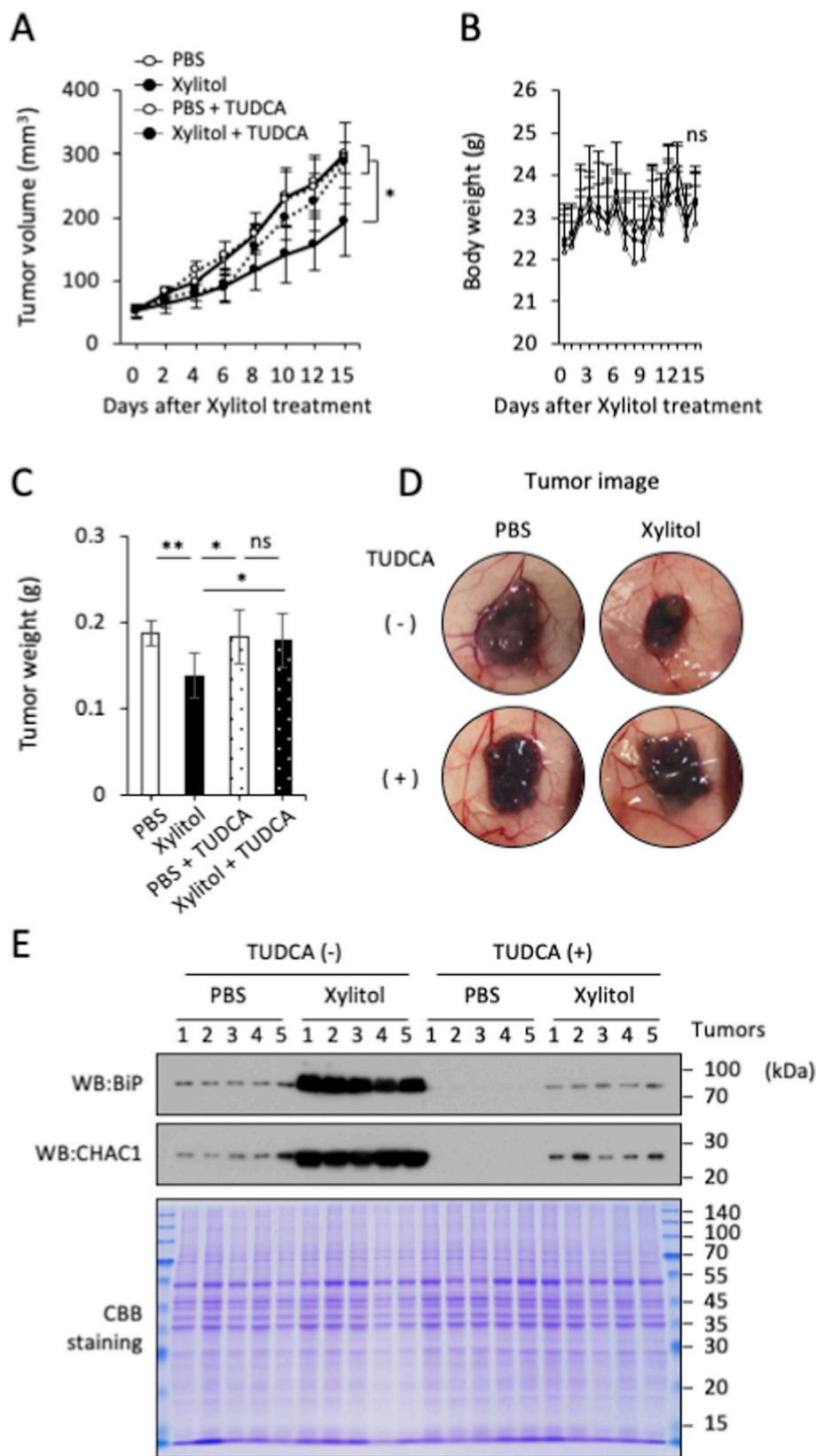


Fig. 5. The ER stress-dependent tumor-suppressive function of xylitol *in vivo*. **A–D:** MeWo cell-derived tumor sizes were monitored on the indicated days. Xylitol (2.0 g/kg in PBS) was administered via the tail vein starting at day 0 (the tumor volumes reached approx. 50–100 mm³) and then daily (A). Regarding panel (A), the ER-stress inhibitor TUDCA (250 mg/kg in PBS) was further intraperitoneally administered to PBS- or xylitol-treated mice starting on day 7, and the mice underwent the same injection every other day (A). In parallel with (A), body weights were also monitored (B). Tumor weights were quantified (C) and tumor images were taken (D) 15 days after the administration. (E) On day 15, the resected tumors were collected, lysed, and subjected to SDS-PAGE, and then the protein levels of BiP and CHAC1 were evaluated by western blots. *Bottom:* CBB staining showing the internal control and proper loading of the protein specimens. Data are mean ± SD. ns, not significant; *p < 0.05, **p < 0.01, ***p < 0.001 by Student's *t*-test.

that xylitol might not affect the glycolysis process in tumors *in vivo*.

Notably, although in the PBS-treated mice the tissue surrounding the tumor front had become very rough, representing a highly invasive tumor phenotype, the tumor front in the xylitol-treated cases was very smooth, suggesting that xylitol has an ability to suppress not only

cancer growth but also cancer invasiveness (Fig. 4F). In this setting, we also examined the induction of ER stress and the subsequent CHAC1 status *in vivo*. We detected a significant accumulation of BiP as well as CHAC1 in the xylitol-treated tumor groups in a common manner that occurred specifically in the intravenous administration but not the oral

administration (Fig. 4G).

ER stress is also likely to play a crucial role in the xylitol-induced tumor suppression in *in vivo* settings just as it does in *in vitro* settings. We therefore used the major ER-stress inhibitor TUDCA in the same experiment, as TUDCA may cancel the effect of xylitol. TUDCA was used at 250 mg/kg since this concentration has been reported as an effective dose that works sufficiently in a mouse model [12]. As expected, TUDCA effectively canceled the xylitol-mediated tumor

suppression (Fig. 5A). The body weights of the mice were not affected by any of the treatments in the experiment (Fig. 5B). On day 15, the tumor weights in the xylitol-treated groups had caught up to almost the same levels as those of the PBS-treated tumor groups (Fig. 5C).

Our examination of the tumor images derived from each group revealed a smooth interface representing non-aggressiveness only in the xylitol-treated groups; this phenotype turned into an aggressive phenotype after xylitol was combined with TUDCA (Fig. 5D). The results

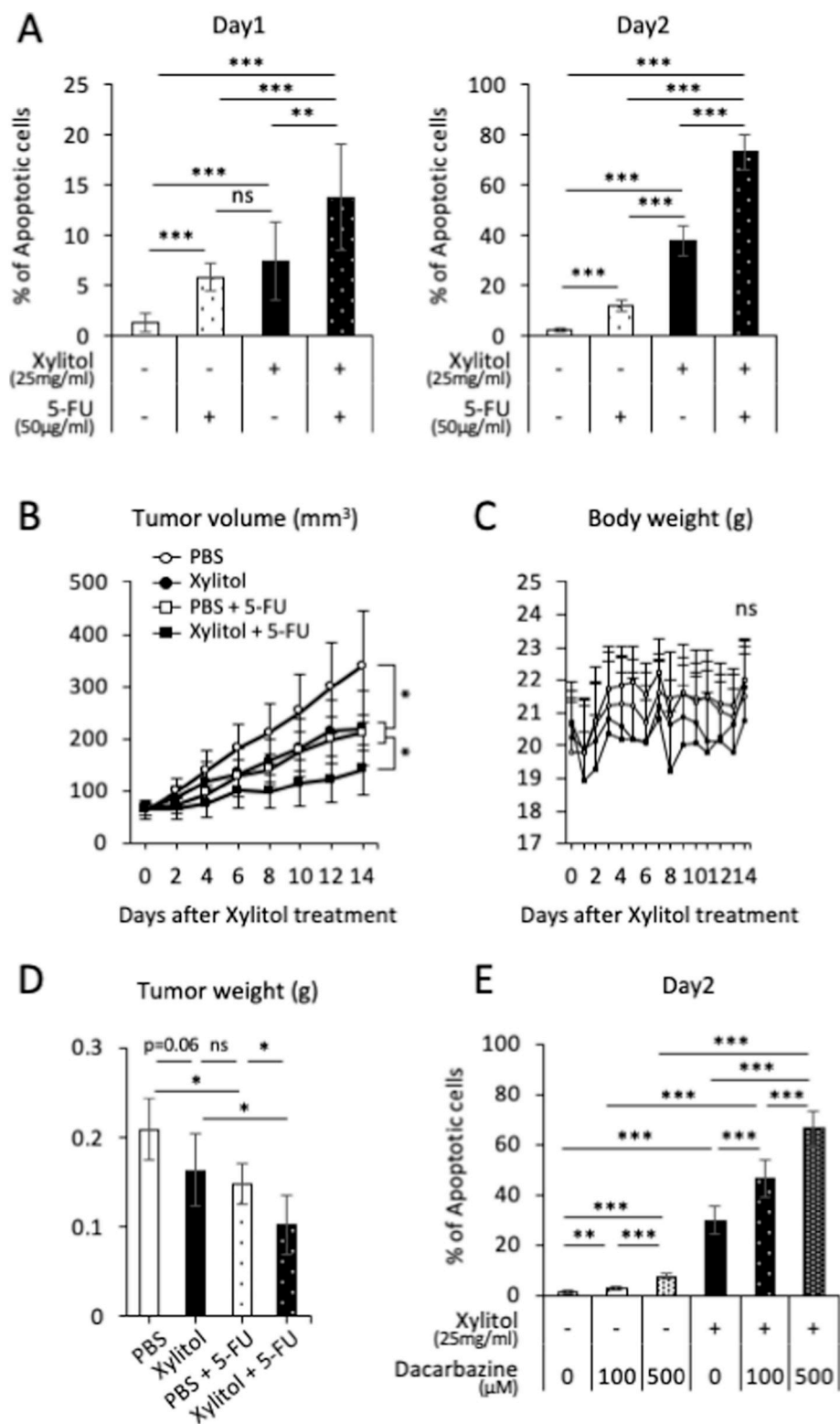


Fig. 6. The increased tumor-suppressive function of 5-FU by blending with xylitol. **A:** MeWo cells were treated with 5-FU (50 µg/ml) in the presence or absence of xylitol (25 mg/ml). After 24-h (*left*) or 48-h (*right*) treatment of the cells, *in vitro* apoptotic assessments were carried out. **B–D:** MeWo cell-derived tumor sizes (**B**) and body weights (**C**) were monitored on the indicated days after the administration of xylitol (2.0 g/kg in PBS) combined with or without 5-FU (50 µg/kg) or single 5-FU (50 µg/kg) via the tail vein starting at day 0 and then daily for xylitol and weekly for 5-FU. Tumor weights were quantified (**D**) 14 days after the administration. **E:** MeWo cells were treated with dacarbazine (0, 100, or 500 µM) in the presence or absence of xylitol (25 mg/ml). After 48-h treatment of the cells, *in vitro* apoptotic assessments were carried out. Data are mean ± SD. ns, not significant; *p < 0.05, **p < 0.01, ***p < 0.001 by Student's *t*-test.

also confirmed that TUDCA efficiently blocked both the BiP induction and CHAC1 induction caused by xylitol (Fig. 5E). These results indicate that xylitol has a tumor-suppressive function when intravenously administered, and this function is dependent on the presence of some level of ER stress.

3.5. Xylitol sensitized melanoma cells to chemotherapeutic drugs

The oxidative stress caused by the xylitol-mediated glutathione reduction may enhance the effect of chemotherapeutic drugs. In fact, our previous study demonstrated that xylitol markedly reinforces the cordycepin-mediated apoptosis of cancer cells [2]. We examined this further herein. As expected, xylitol effectively sensitized melanoma cells to a 5-FU anticancer chemical *in vitro* (Fig. 6A) as well as *in vivo* (Fig. 6B–D). The *in vitro* sensitization effect of xylitol was also observed for another compound, dacarbazine, which is clinically approved for treating melanoma (Fig. 6E). Our results thus suggest that xylitol enhances the effects of chemotherapeutic drugs for cancer prevention.

4. Discussion

4.1. Molecules associated with the apoptotic machinery triggered by xylitol in cancer cells

Our present findings demonstrated that xylitol has a prominent cancer-suppressing ability in an *in vitro* cell culture system as well as in an *in vivo* cancer-bearing mouse model. In the mouse model, the oral administration of xylitol had no effect on the cancer suppression, whereas the intravenous injection of xylitol prevented cancer growth, probably due to some type of acid-mediated inactive modification or degradation of xylitol; otherwise, there would be an insufficient absorbance of xylitol into the blood by way of the oral-gastric route. Our mechanistic studies also showed that xylitol-mediated cancer apoptosis was triggered by the upregulation of CHAC1 (which originates in ATF4 activation via xylitol-triggered ER stress), eventually leading to oxidative stress since CHAC1 enzymatically degrades intracellular glutathione [14–16].

We examined these events mainly in MeWo cells, and some key findings were confirmed in other types of cancer cells (e.g., PANC-1 cells, AsPC-1 and MIA PaCa-2 cells) (Supplementary Fig. S4), and thus our proposed pathway is not restricted to only a single cell line. On the other hand, the xylitol-mediated apoptotic pathway as described above does not appear to be involved in normal human OUMS-24 fibroblasts, suggesting that xylitol could be an effective and useful daily food component for preventing cancers in a selective manner.

Here, our primary question was whether the xylitol-mediated apoptotic cell death is explained by CHAC1 alone. As shown by the results of the RNA-seq-based analysis (Fig. 1C), in addition to CHAC1, other molecules that may be related to apoptosis and growth regulation, such as HIPK2, MAFK, RERE, BCAP29, MRPL34, PIR and RPP21, attracted our attention. However, the reproducibility of their inductions by xylitol treatment was not shown by the confirmation study based on the quantitative real-time PCR analysis results (Fig. 1D), and we thus omitted these genes from the xylitol pathway. We speculate that there is no close link between CHAC1 and the omitted individual genes. In addition, we did not observe any association between ER stress and these omitted genes (except for HIPK2) in our review of the relevant published studies. Lee et al. reported that ER stress-mediated neurodegeneration in amyotrophic lateral sclerosis (ALS) is promoted by the induced HIPK2 [19]. This may indicate that xylitol-mediated ER stress is different in nature from the ER-stress caused by ALS disease.

Our second question concerned the results provided in Fig. 2D: why did the decrease of CHAC1 expression induced by the siRNA cause a moderate suppression of the xylitol-induced ROS production in MeWo cells? This result may indicate that ER stress-mediated CHAC1 is not the only source of ROS in the xylitol-treated cells. Similarly, CHAC1

induction may not be the only event responsible for the anticancer properties of xylitol, as shown in the *in vivo* studies. Because quite a few molecules would be regulated by xylitol-mediated ER stress, it is surely possible that molecule(s) other than CHAC1 also contribute to the xylitol-mediated anticancer machinery. In this study, our experiments searching for important molecules involved in the control of xylitol-mediated cancer apoptosis were only conducted at the RNA level. Since mRNA expressions do not always reflect the corresponding protein levels, comprehensive analyses at the protein level could lead to the identification of additional important regulators that will clarify the CHAC1-integrated or not-integrated mechanism(s) of the anticancer role of xylitol. This subject is part of our ongoing research.

4.2. Xylitol-mediated ER stress

In the context of the mechanism proposed above, it is not yet known how ER stress is exerted by xylitol incorporation in cancer cells. Intracellular metabolite(s) of xylitol may provide a clue. One of the xylitol metabolites, xylulose-5-P, was reported to be able to inhibit the glycolysis system in mammalian cells [20]. Thereby, the glycolysis-produced ATP level may be significantly reduced by xylitol, since ATP is required for protein folding. However, we observed that xylitol did not consume ATP at a much higher level in the treated cells (Figs. 1B and 2D), and in our additional studies, the xylitol-derived apoptotic cell death was not affected by a hypoxic environment that shifts the mitochondria-based ATP production to glycolysis-based ATP production (data not shown).

In light of those findings and reports, we speculated that xylitol might disturb the normal protein glycosylation in the ER. Because xylitol is of plant origin, it may compete with glucose or another monosaccharide that is used for several glycosylation reactions of proteins in the ER. Our prior relevant data showed that the glycosylation state is altered by xylitol treatment (data not shown), and this may be followed by a marked increase in misfolded proteins that are linked to ER stress. This idea may be supported by the finding that a major ER-stress inducer, tunicamycin, mediated the incomplete glycosylation of proteins that can readily induce protein misfolding [21].

4.3. Xylitol exerts selective apoptotic cell death in cancer cells

Another question is why cancer selectivity exists for the xylitol-mediated ER stress. This may be explained by an increase of xylitol uptake in cancer cells in comparison to that in normal cells. This may be similar to the case of glucose uptake in cancer cells, since monosaccharide glucose is highly incorporated into many types of cancer cells due to the significantly elevated expression of glucose membrane transporters. The glucose transporters belong to the family of solute carrier *SLC* genes. Since xylitol transporter(s) are probably present in the same gene family, we are now attempting to identify xylitol-specific transporter(s) that are clearly expressed in cancer cells from among the *SLC* family members (423 genes); we have narrowed down the candidates to seven candidates.

However, we should not disregard another possible explanation for the different reactions to xylitol between normal cells and cancer cells. This may be explained by the differences in the intracellular behaviors of xylitol and its metabolites in the cells, since a series of enzymes that play a part in catalyzing xylitol are inevitably present in different states of expression and activity in the individual cell types. Molecules that have resistant functions to ER stress or apoptosis may also contribute. Taken together, the present and past findings highlight the need for further comprehensive analyses including membrane transporters, xylitol metabolites and intracellular proteins to expand our understanding of the complex mechanism(s) of xylitol sensitivity and resistance, which may explain how cells acquire xylitol selectivity or specificity.

4.4. Xylitol may sensitize cancer stem cells to chemotherapeutic drugs

Our data also show that the anticancer effect of xylitol is moderate but that xylitol has a definite ability to enhance the effects of common anticancer drugs such as 5-FU [22] when combined with them. Thus, the control of glutathione at a low level that induces oxidative stress in a cancer-selective manner may greatly contribute to the effects of anticancer drugs. In addition, the strategy of maintaining the intracellular glutathione at a low level provides a great benefit when we target cancer stem cells, since cell surface membrane protein CD44 variant isoform (CD44v)-positive cancer stem cells frequently show much higher levels of glutathione due to the enhanced uptake of materials (e.g., cysteine and glutamate) that are used to make glutathione, and thereby cancer stem cells display quite high resistance to the oxidative stress caused by chemotherapeutic drugs [23].

It was reported that an inhibitor of xCT (another glutathione regulator that functions as a cysteine and glutamate transporter, whose activity is upregulated by the interaction with CD44v), *i.e.*, sulfasalazine, suppresses CD44v-positive cancer stem cell growth [23]. The antitumor effect of cisplatin at a low dose (2 mg/kg) was significantly enhanced by treatment with sulfasalazine. Taken together, these results indicate that not only sulfasalazine but also xylitol reduces the ROS defense capacity of cancer cells (including cancer stem cells) and sensitizes them to chemotherapeutic drugs.

4.5. Xylitol may prevent cancer invasion and metastasis

Xylitol may have another ability to prevent important cancer events such as cancer metastasis. Regarding cancer inflammation, using our melanoma dissemination model and our subsequent lung metastasis model, we previously demonstrated that S100A8/A9 (a heterodimer complex of S100A8 and S100A9) plays a crucial role in melanoma metastasis [24–33]. This protein has an interesting feature of high secretion in melanomas that surround skin stroma and remote lung sites. We previously demonstrated that S100A8/A9 at melanomas surrounding stroma in the skin strongly stimulate melanoma invasion, leading to local dissemination [32]. The melanoma-mediated S100A8/A9 secretion from the lung also stimulates the disseminated melanoma in the skin to metastasize to the lung, resulting in lung tropic metastasis.

Herein, to examine this additional therapeutic benefit of xylitol, we investigated S100A8/A9 induction in xylitol-treated melanoma-bearing mice, and we observed that xylitol shows a trend of preventing S100A8/A9 induction in the lung (Supplementary Fig. S6). We also observed a major difference in the inoculated tumor surfaces between the xylitol-treated and not-treated mice, *i.e.*, smooth versus rough surfaces (Figs. 4F and 5D). The rough surface represents an aggressively infiltrating phenotype of melanoma, probably caused by surrounding S100A8/A9, whereas xylitol may suppress S100A8/A9 induction in the melanoma skin area, eventually leading to the prevention of the local dissemination.

It has also been reported that xylitol efficiently blocked inflammation [34]. Because inflammation readily induces S100A8/A9, the blocking of S100A8/A9 induction by treatment with xylitol may provide another therapeutic benefit against cancer. In the present study, we were not able to determine whether xylitol can prevent cancer metastasis. This is because our mouse model used herein is not suitable as an evaluation model of cancer metastasis; in addition, the shorter evaluation schedule was not long enough to induce cancer metastasis from the developed tumor area. We have only speculation based on the results of the analysis of S100A8/A9 in the lung combined with our findings [24–33] and those of others [34] as mentioned above. We are planning to thoroughly investigate the anti-metastatic effect of xylitol in an optimal mouse model in the future, based on our current findings regarding S100A8/A9-mediated cancer metastasis.

5. Conclusion

In conclusion, our results support the notion that xylitol has a tumor-suppressive function that acts via oxidative stress, which is caused by the xylitol-triggered ER stress, by which a marked level of CHAC1 is induced and reduces cellular glutathione. The xylitol-mediated oxidative stress greatly contributes to an enhancement of the anticancer effect of the chemotherapeutic drug 5-FU *in vitro* as well as *in vivo*. Taken together, our past and present findings indicate that the use of xylitol as an adjunct to chemotherapy may be an effective approach for improving therapeutic outcomes, similarly to sulfasalazine.

Funding

This work was supported by a collaboration grant from the Cordyceps militaris Project from CAITAC Corp. (Okayama, Japan) to M.S. and by research grants from the Kobayashi Foundation and the Smoking Research Foundation to M.S.

CRediT authorship contribution statement

Nahoko Tomonobu: Conceptualization, Data curation, Formal analysis, Investigation, Methodology, Writing - original draft. **Ni Luh Gede Yoni Komalasari:** Formal analysis. **I Wayan Sumardika:** Formal analysis. **Fan Jiang:** Formal analysis. **Youyi Chen:** Formal analysis. **Ken-ichi Yamamoto:** Formal analysis. **Rie Kinoshita:** Formal analysis. **Hitoshi Murata:** Formal analysis. **Yusuke Inoue:** Formal analysis, Validation. **Masakiyo Sakaguchi:** Conceptualization, Funding acquisition, Methodology, Project administration, Supervision, Writing - original draft, Writing - review & editing.

Declaration of competing interest

The authors declare that they have no known competing financial interests or personal relationships that could have appeared to influence the work reported in this paper.

Appendix A. Supplementary data

Supplementary data to this article can be found online at <https://doi.org/10.1016/j.cbi.2020.109085>.

References

- [1] I.M. Ruma, E.W. Putranto, E. Kondo, R. Watanabe, K. Saito, Y. Inoue, K. Yamamoto, S. Nakata, M. Kaihata, H. Murata, M. Sakaguchi, Extract of Cordyceps militaris inhibits angiogenesis and suppresses tumor growth of human malignant melanoma cells, *Int. J. Oncol.* 45 (2014) 209–218.
- [2] T. Wada, I.W. Sumardika, S. Saito, I.M.W. Ruma, E. Kondo, M. Shibukawa, M. Sakaguchi, Identification of a novel component leading to anti-tumor activity besides the major ingredient cordycepin in Cordyceps militaris extract, *J. Chromatogr. B Analyt. Technol. Biomed. Life Sci.* 1061–1062 (2017) 209–219.
- [3] S.K. Das, M. Masuda, A. Sakurai, M. Sakakibara, Medicinal uses of the mushroom Cordyceps militaris: current state and prospects, *Fitoterapia* 81 (2010) 961–968.
- [4] H.S. Tuli, A.K. Sharma, S.S. Sandhu, D. Kashyap, Cordycepin: a bioactive metabolite with therapeutic potential, *Life Sci.* 93 (2013) 863–869.
- [5] K. Nakamura, K. Shinozuka, N. Yoshikawa, Anticancer and antimetastatic effects of cordycepin, an active component of Cordyceps sinensis, *J. Pharmacol. Sci.* 127 (2015) 53–56.
- [6] R. Ohashi, M. Miyazaki, K. Fushimi, T. Tsuji, Y. Inoue, N. Shimizu, M. Namba, Enhanced activity of cyclin A-associated kinase in immortalized human fibroblasts, *Int. J. Canc.* 82 (1999) 754–758.
- [7] E. Park, M.H. Park, H.S. Na, J. Chung, Xylitol induces cell death in lung cancer A549 cells by autophagy, *Biotechnol. Lett.* 37 (2015) 983–990.
- [8] W. Pool, D. Hane, Acute Toxicity and Dog Tolerance Testing of Xylitol. Unpublished Report from the Research Department of Hoffmann La Roche Co., Submitted to World Health Organisation by Hoffmann, La Roche Co., Basle, Switzerland, 1970.
- [9] D. Schadendorf, K. Jurgovsky, M. Worm, B.M. Czarnetzki, In vitro sensitivity of human melanoma cells to chemotherapeutic agents and interferons, *Melanoma Res.* 4 (1994) 243–249.
- [10] S. Nishikawa, M. Naya, T. Hara, H. Miyazaki, Y. Ohguro, Safety evaluation of DITC acute toxicity (mice, rats), *Yakuri To Chiryō* 9 (1981) 3105–3109.

- [11] B. Schmidt, N. Fingerhut, K. Lang, Über den stoffwechsel von radioaktiv markiertem xylitol bei der ratte, *Klin. Wochenschr.* 42 (1964) 1073–1077 (In German).
- [12] C. Rubio-Patiño, J.P. Bossowski, G.M.D. Donatis, L. Mondragón, E. Villa, L.E. Aira, J. Chiche, R. Mhaidly, C. Lebeaupin, S. Marchetti, K. Voutetakis, A. Chatziioannou, F.A. Castelli, P. Lamourette, E. Chu-Van, F. Fenaillé, T. Avril, T. Passeron, J.B. Patterson, E. Verhoeyen, B. Bailly-Maitre, E. Chevet, J.E. Ricci, Low-protein diet induces IRE1 α -dependent anticancer immunosurveillance, *Cell Metabol.* 27 (2018) 828–842.
- [13] Y.M. Yoon, J.H. Lee, S.P. Yun, Y.S. Han, C.W. Yun, H.J. Lee, H. Noh, S.J. Lee, H.J. Han, S.H. Lee, Tauroursodeoxycholic acid reduces ER stress by regulating of Akt-dependent cellular prion protein, *Sci. Rep.* 22 (2016) 39838.
- [14] R.R. Crawford, E.T. Prescott, C.F. Sylvester, A.N. Higdon, J. Shan, M.S. Kilberg, I.N. Mungroe, Human CHAC1 protein degrades glutathione, and mRNA induction is regulated by the transcription factors ATF4 and ATF3 and a bipartite ATF/CRE regulatory element, *J. Biol. Chem.* 290 (2015) 15878–15891.
- [15] N. Wang, G.Z. Zeng, J.L. Yin, Z.X. Bian, Artesunate activates the ATF4-CHOP-CHAC1 pathway and affects ferroptosis in Burkitt's lymphoma, *Biochem. Biophys. Res. Commun.* 519 (2019) 533–539.
- [16] D. Scheffer, G. Kulcsár, G. Nagyéri, M. Kiss-Merki, Z. Rékási, M. Maloy, T. Czömpöly, Active mixture of serum-circulating small molecules selectively inhibits proliferation and triggers apoptosis in cancer cells via induction of ER stress, *Cell. Signal.* 65 (2019) 109426.
- [17] H. Malhi, R.J. Kaufman, Endoplasmic reticulum stress in liver disease, *J. Hepatol.* 54 (2011) 795–809.
- [18] J. Sato, Y.-M. Wang, J.v. Eys, Metabolism of xylitol and glucose in rats bearing hepatocellular carcinomas, *Canc. Res.* 41 (1981) 3192–3199.
- [19] S. Lee, Y. Shang, S.A. Redmond, A. Urisman, A.A. Tang, K.H. Li, A.L. Burlingame, R.A. Pak, A. Jovičić, A.D. Gitler, J. Wang, N.S. Gray, W. W Seeley, T. Siddique, E.H. Bigio, V.M. Lee, J.Q. Trojanowski, J.R. Chan, E.J. Huang, Activation of HIPK2 promotes ER stress-mediated neurodegeneration in amyotrophic lateral sclerosis, *Neuron* 91 (2016) 41–55.
- [20] K. Iizuka, W. Wu, Y. Horikawa, J. Takeda, Role of glucose-6-phosphate and xylulose-5-phosphate in the regulation of glucose-stimulated gene expression in the pancreatic β cell line, INS-1E, *Endocr. J.* 60 (2013) 473–482.
- [21] P. Guha, E. Kaptan, P. Gade, D.V. Kalvakolanu, H. Ahmed, Tunicamycin induced endoplasmic reticulum stress promotes apoptosis of prostate cancer cells by activating mTORC1, *Oncotarget* 8 (2017) 68191–68207.
- [22] Y.W. Naguib, A. Kumar, Z. Cui, The effect of microneedles on the skin permeability and antitumor activity of topical 5-fluorouracil, *Acta Pharm. Sin. B* 4 (2014) 94–99.
- [23] T. Ishimoto, O. Nagano, T. Yae, M. Tamada, T. Motohara, H. Oshima, M. Oshima, T. Ikeda, R. Asaba, H. Yagi, T. Masuko, T. Shimizu, T. Ishikawa, K. Kai, E. Takahashi, Y. Imamura, Y. Baba, M. Ohmura, M. Suematsu, H. Baba, H. Saya, CD44 variant regulates redox status in cancer cells by stabilizing the xCT subunit of system xc(-) and thereby promotes tumor growth, *Canc. Cell* 19 (2011) 387–400.
- [24] T. Hibino, M. Sakaguchi, S. Miyamoto, M. Yamamoto, A. Motoyama, J. Hosoi, T. Shimokata, T. Ito, R. Tsuboi, N.H. Huh, S100A9 is a novel ligand of EMMPRIN that promotes melanoma metastasis, *Canc. Res.* 73 (2013) 172–183.
- [25] I.M. Ruma, E.W. Putranto, E. Kondo, H. Murata, M. Watanabe, P. Huang, R. Kinoshita, J. Futami, Y. Inoue, A. Yamauchi, I.W. Sumardika, C. Youyi, K. Yamamoto, Y. Nasu, M. Nishibori, T. Hibino, M. Sakaguchi, MCAM, as a novel receptor for S100A8/A9, mediates progression of malignant melanoma through prominent activation of NF- κ B and ROS formation upon ligand binding, *Clin. Exp. Metastasis* 33 (2016) 609–627.
- [26] M. Sakaguchi, S100-SPECT uncovers cellular and molecular events of pre-metastatic niche formation and following organ-specific cancer metastasis, *Theranostics* 7 (2017) 2649–2651.
- [27] I.W. Sumardika, C. Youyi, E. Kondo, Y. Inoue, I.M.W. Ruma, H. Murata, R. Kinoshita, K.I. Yamamoto, S. Tomida, K. Shien, H. Sato, A. Yamauchi, J. Futami, E.W. Putranto, T. Hibino, S. Toyooka, M. Nishibori, M. Sakaguchi, β -1,3-Galactosyl-O-glycosyl-glycoprotein β -1,6-N-acetylglucosaminyltransferase 3 increases MCAM stability, which enhances S100A8/A9-mediated cancer motility, *Oncol. Res.* 26 (2018) 431–444.
- [28] R. Kinoshita, H. Sato, A. Yamauchi, Y. Takahashi, Y. Inoue, I.W. Sumardika, Y. Chen, N. Tomonobu, K. Araki, K. Shien, S. Tomida, H. Torigoe, K. Namba, E. Kurihara, Y. Ogoshi, H. Murata, K.I. Yamamoto, J. Futami, E.W. Putranto, I.M.W. Ruma, H. Yamamoto, J. Soh, T. Hibino, M. Nishibori, E. Kondo, S. Toyooka, M. Sakaguchi, exSSSRs (extracellular S100 soil sensor receptors)-Fc fusion proteins work as prominent decoys to S100A8/A9-induced lung tropic cancer metastasis, *Int. J. Canc.* 144 (2019) 3138–3145.
- [29] R. Kinoshita, H. Sato, A. Yamauchi, Y. Takahashi, Y. Inoue, I.W. Sumardika, Y. Chen, N. Tomonobu, K. Araki, K. Shien, S. Tomida, H. Torigoe, K. Namba, E. Kurihara, Y. Ogoshi, H. Murata, K.I. Yamamoto, J. Futami, E.W. Putranto, I.M.W. Ruma, H. Yamamoto, J. Soh, T. Hibino, M. Nishibori, E. Kondo, S. Toyooka, M. Sakaguchi, Newly developed anti-S100A8/A9 monoclonal antibody efficiently prevents lung tropic cancer metastasis, *Int. J. Canc.* 145 (2019) 569–575.
- [30] I.W. Sumardika, Y. Chen, N. Tomonobu, R. Kinoshita, I.M.W. Ruma, H. Sato, E. Kondo, Y. Inoue, A. Yamauchi, H. Murata, K.I. Yamamoto, S. Tomida, K. Shien, H. Yamamoto, J. Soh, J. Futami, E.W. Putranto, T. Hibino, M. Nishibori, S. Toyooka, M. Sakaguchi, Neuroplastin- β mediates S100A8/A9-induced lung cancer dissemination progression, *Mol. Carcinog.* 58 (2019) 980–995.
- [31] N. Tomonobu, R. Kinoshita, I.W. Sumardika, Y. Chen, Y. Inoue, A. Yamauchi, K.I. Yamamoto, H. Murata, M. Sakaguchi, Convenient methodology for extraction and subsequent selective propagation of mouse melanocytes in culture from adult mouse skin tissue, *Biochem. Biophys. Rep.* 18 (2019) 100619.
- [32] Y. Chen, I.W. Sumardika, N. Tomonobu, I.M.W. Ruma, R. Kinoshita, E. Kondo, Y. Inoue, H. Sato, A. Yamauchi, H. Murata, K.I. Yamamoto, S. Tomida, K. Shien, H. Yamamoto, J. Soh, M. Liu, J. Futami, K. Sasai, H. Katayama, M. Kubo, E.W. Putranto, T. Hibino, B. Sun, M. Nishibori, S. Toyooka, M. Sakaguchi, Melanoma cell adhesion molecule is the driving force behind the dissemination of melanoma upon S100A8/A9 binding in the original skin lesion, *Canc. Lett.* 452 (2019) 178–190.
- [33] Y. Chen, I.W. Sumardika, N. Tomonobu, R. Kinoshita, Y. Inoue, H. Iioka, Y. Mitsui, K. Saito, I.M.W. Ruma, H. Sato, A. Yamauchi, H. Murata, K.I. Yamamoto, S. Tomida, K. Shien, H. Yamamoto, J. Soh, J. Futami, M. Kubo, E.W. Putranto, T. Murakami, M. Liu, T. Hibino, M. Nishibori, E. Kondo, S. Toyooka, M. Sakaguchi, Critical role of the MCAM-ETV4 axis triggered by extracellular S100A8/A9 in breast cancer aggressiveness, *Neoplasia* 21 (2019) 627–640.
- [34] E. Park, H.S. Na, S.M. Kim, S. Wallet, S. Cha, J. Chung, Xylitol, an anticaries agent, exhibits potent inhibition of inflammatory responses in human THP-1-derived macrophages infected with *Porphyromonas gingivalis*, *J. Periodontol.* 85 (2014) e212–223.